Diffraction by Arbitrary-angled Dielectric Wedges: Closed Form High-Frequency Solutions

M. Frongillo[1], **G. Gennarelli**[2], **and G. Riccio**[1]

[1]D.I.E.M., University of Salerno, Via Giovanni Paolo II 132, Fisciano (SA) 84084, Italy
[2]Institute for Electromagnetic Sensing of the Environment, National Research Council
Via Diocleziano 328, Naples 80124, Italy

Abstract— Diffraction inside and outside an arbitrary-angled lossless penetrable wedge is considered in this study. Closed form expressions are presented for the diffracted field in the inner region of the wedge and the surrounding space in the case of E-polarized incident plane waves. They are obtained by performing a uniform asymptotic evaluation of the radiation integrals arising from the use of a physical optics approximation for the equivalent electric and magnetic surface currents lying on the inner and outer wedge faces. Good accuracy in the evaluation of the total field, ease of use and implementation in a computer code are the advantages of the proposed solutions, which permit to compensate the geometrical optics discontinuities.

1. INTRODUCTION

Uniform Asymptotic Physical Optics (UAPO) solutions were proposed in explicit closed form by the authors in [1] and [2] for evaluating the field diffracted by right- and obtuse-angled lossless dielectric wedges in the inner and outer regions. In addition, the corresponding time domain diffraction coefficients were derived in [3] and [4] via an inverse Laplace transform. Their knowledge allows one to evaluate (via a convolution integral) the transient diffracted field originated by an arbitrary function plane wave impinging on the wedge. The UAPO-based approach in the frequency domain has been also applied to acute-angled wedges [5] considering a specific range of incidence directions. The UAPO solutions were able to compensate the Geometrical Optics (GO) discontinuities, accurate when compared with available numerical tools, and easy to handle since expressed in terms of the GO response of the structure and the transition function of the Uniform Theory of Diffraction (UTD) [6]. On the other hand, the use of a PO approximation implies inaccuracies in the case of grazing incidence and in correspondence of the dielectric interfaces.

This research contribution is devoted to extend the analysis in [5] to all possible cases of plane wave incidence and to provide generalized UAPO solutions, which can be applied to the diffraction by a wedge with arbitrary apex angle. Such solutions include those proposed in [1, 2, 5] as particular cases and are obtained accounting for the equivalent electric and magnetic PO current densities on the internal and external faces of the wedge. Multiple internal reflections and external transmissions are considered for their explicit evaluation by varying the direction of the incident plane wave. Numerical tests confirm the effectiveness of the proposed UAPO solutions for the field diffracted in the dielectric wedge-shaped region and the surrounding free-space.

2. UAPO DIFFRACTED FIELD

A lossless non-magnetic ($\mu_r = 1$) wedge-shaped region is considered with relative permittivity ε_r and propagation constant $k_d = k_0\sqrt{\varepsilon_r}$, k_0 being the free-space wavenumber. Its surfaces are S_0 and S_n, and the internal apex angle α is assumed less than $\pi/2$ (see Fig. 1). The incidence direction is perpendicular to the edge and defined by ϕ', while the observation point is $P(\rho,\phi)$. The wedge is illuminated by the incident electric field $\underline{E}^i = E_0^i \mathrm{e}^{-j\underline{k}_0\cdot\underline{r}}\hat{z}$ (E-polarization).

The approach for obtaining the UAPO diffracted field is the same used in [1, 2, 5], and neglects the surface waves. Two separate diffraction problems are solved by formulating the corresponding radiation integrals in terms of electric and magnetic equivalent PO surface currents on the internal and external faces of the wedge.

2.1. $0 < \phi' < \pi/2$

If $\theta^i = \pi/2 - \phi'$ is the external incidence angle, the waves penetrate into the wedge through S_0 with the transmission angle $\theta_{0L}^t = \sin^{-1}(\sin\theta^i/\sqrt{\varepsilon_r})$, and travel toward the apex undergoing N reflections/transmissions before moving away from it. A crucial interaction point is that corresponding to the internal incidence angle $\theta_{N+1}^i = (N+1)\,\alpha - \theta_{0L}^t = \theta_{0R}^t$. Accordingly, the number of total internal reflections is $N + M + 1$, where $M = \mathrm{Int}\left[(\pi/2 - \theta_{0R}^t)/\alpha\right]$. Transmitted waves through S_0 and S_n exist until the total reflection occurs inside the wedge.

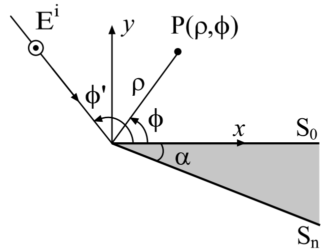

Figure 1: Geometry of the problem.

2.1.1. Internal Region

$$\underline{E}^d_{int}(P) = \left[D^{int}_L + D^{int}_R\right] \frac{e^{-jk_d\rho}}{\sqrt{\rho}} E^i_0 \hat{z} = \left[\left(D^{int}_L\right)_{S_0} + \left(D^{int}_L\right)_{S_n} + \left(D^{int}_R\right)_{S_0} + \left(D^{int}_R\right)_{S_n}\right] \frac{e^{-jk_d\rho}}{\sqrt{\rho}} E^i_0 \hat{z} \quad (1)$$

with

$$\left(D^{int}_L\right)_{S_0} = \frac{e^{-j\pi/4}}{2\sqrt{2\pi k_d}} T_0 B\left(N, \theta^t_{0L}, \theta^i_n, \rho, \phi\right); \quad \left(D^{int}_R\right)_{S_0} = \frac{e^{-j\pi/4}}{2\sqrt{2\pi k_d}} T_0 \Gamma(N) B\left(M, -\theta^t_{0R}, -\theta^i_m, \rho, \phi\right) \quad (2)$$

$$\left(D^{int}_L\right)_{S_n} = \frac{e^{-j\pi/4}}{2\sqrt{2\pi k_d}} T_0 B'\left(N, \theta^i_n, \rho, \phi\right); \quad \left(D^{int}_R\right)_{S_n} = \frac{e^{-j\pi/4}}{2\sqrt{2\pi k_d}} T_0 \Gamma(N) B'\left(M, -\theta^i_m, \rho, \phi\right) \quad (3)$$

where T_0 is the transmission coefficient at the free space/dielectric interaction, $\Gamma(N)$ represents the product of the internal reflection coefficients R, $\theta^i_n = \theta^t_{0L} - n\,\alpha$, $\theta^i_m = \theta^t_{0R} + m\alpha$. Moreover,

$$\begin{aligned} B\left(L, \theta^t_0, \theta^i_l, \rho, \phi\right) = & \left(\sin\phi - \cos\theta^t_0\right) F\left(k_d, \rho, 2\pi - \phi, \frac{\pi}{2} - \theta^t_0\right) \\ & + \sum_{\substack{l=1 \\ l\,even}}^{L} \left(\prod_{p=1}^{l-1} R_p\right) \left[(1 + R_l)\sin\phi + (1 - R_l)\cos\theta^i_l\right] F\left(k_d, \rho, 2\pi - \phi, \frac{\pi}{2} - \theta^i_l\right) \end{aligned} \quad (4)$$

$$B'\left(L, \theta^i_l, \rho, \phi\right) = \sum_{\substack{m=1 \\ m\,odd}}^{L} \left(\prod_{p=1}^{l-1} R_p\right) \left[(1 - R_l)\cos\theta^i_l - (1 + R_l)\sin(\phi + \alpha)\right] F\left(k_d, \rho, \phi - (2\pi - \alpha), \frac{\pi}{2} - \theta^i_l\right) \quad (5)$$

where

$$F(k, \rho, u, \pm v) = \frac{F_t\left(2k\rho\cos^2\left(\frac{u \pm v}{2}\right)\right)}{\cos u + \cos v} \quad (6)$$

and $F_t(\cdot)$ is the standard UTD transition function [6].

2.1.2. External Region

$$\underline{E}^d_{ext}(P) = \left[\left(D^{ext}_L\right)_{S_0} + \left(D^{ext}_L\right)_{S_n} + \left(D^{ext}_R\right)_{S_0} + \left(D^{ext}_R\right)_{S_n} + DI + DR\right] \frac{e^{-jk_0\rho}}{\sqrt{\rho}} E^i_0 \hat{z} \quad (7)$$

with

$$\left(D^{ext}_L\right)_{S_0} = -\frac{e^{-j\pi/4}}{2\sqrt{2\pi k_0}} T_0 C\left(N+1, q\theta^t_n, \theta^i_n, \rho, \phi\right); \quad \left(D^{ext}_R\right)_{S_0} = -\frac{e^{-j\pi/4}}{2\sqrt{2\pi k_0}} T_0 \Gamma(N) C\left(M, -\theta^t_m, \theta^i_m, \rho, \phi\right) \quad (8)$$

$$\left(D^{ext}_L\right)_{S_n} = \frac{e^{-j\pi/4}}{2\sqrt{2\pi k_0}} T_0 C'\left(N+1, p\theta^t_n, \theta^i_n, \rho, \phi\right); \quad \left(D^{ext}_R\right)_{S_n} = \frac{e^{-j\pi/4}}{2\sqrt{2\pi k_0}} T_0 \Gamma(N) C'\left(M, -\theta^t_m, \theta^i_m, \rho, \phi\right) \quad (9)$$

$$DI + DR = \left[(1 - R_0)\sin\phi' - (1 + R_0)\sin\phi\right] F\left(k_0, \rho, \phi, \pm\phi'\right) \quad (10)$$

where

$$C\left(L,\theta_l^t,\theta_l^i,\rho,\phi\right)=\sum_{\substack{l=1\\ l\,even}}^{L} T_l\left(\prod_{p=1}^{l-1} R_p\right)\left[\sin\phi+\cos\theta_l^t\right]U\left(\theta_c-\theta_l^i\right)F\left(k_0,\rho,\phi,\pm\left(\frac{\pi}{2}-\theta_l^t\right)\right) \tag{11}$$

$$C'\left(L,\theta_l^t,\theta_l^i,\rho,\phi\right)=\sum_{\substack{l=1\\ l\,odd}}^{L} T_l\left(\prod_{p=1}^{l-1} R_p\right)\left[\sin\left(\phi+\alpha\right)-\cos\theta_l^t\right]U\left(\theta_c-\theta_l^i\right)F\left(k_0,\rho,\left(\phi+\alpha\right),\pm\left(\frac{\pi}{2}-\theta_l^t\right)\right) \tag{12}$$

in which θ_l^t is the transmission angle at the dielectric / free space interactions and $U\left(\theta\right)=1$ if $\theta>0$, 0 elsewhere.

2.2. $\pi/2<\phi'<\pi-\alpha$

The external incidence angle is now $\theta^i=\phi'-\pi/2$. The waves penetrate into the wedge through S_0 with the transmission angle $\theta_{0R}^t=\sin^{-1}(\sin\theta^i/\sqrt{\varepsilon_r})$.

2.2.1. Internal Region

$$\underline{E}_{int}^d\left(P\right)=\left[\left(D_R^{int}\right)_{S_0}+\left(D_R^{int}\right)_{S_n}\right]\frac{e^{-jk_d\rho}}{\sqrt{\rho}}E_0^i\hat{z} \tag{13}$$

with

$$\left(D_R^{int}\right)_{S_0}=\frac{e^{-j\pi/4}}{2\sqrt{2\pi k_d}}\,T_0\,B\left(M,-\theta_{0R}^t,-\theta_m^i,\rho,\phi\right);\quad \left(D_R^{int}\right)_{S_n}=\frac{e^{-j\pi/4}}{2\sqrt{2\pi k_d}}\,T_0\,B'\left(M,-\theta_m^i,\rho,\phi\right) \tag{14}$$

2.2.2. External Region

$$\underline{E}_{ext}^d\left(P\right)=\left[\left(D_R^{ext}\right)_{S_0}+\left(D_R^{ext}\right)_{S_n}+DI+DR\right]\frac{e^{-jk_0\rho}}{\sqrt{\rho}}E_0^i\hat{z} \tag{15}$$

with

$$\left(D_R^{ext}\right)_{S_0}=-\frac{e^{-j\pi/4}}{2\sqrt{2\pi k_0}}\,T_0\,C\left(M,-\theta_m^t,\theta_m^i,\rho,\phi\right);\quad \left(D_R^{ext}\right)_{S_n}=\frac{e^{-j\pi/4}}{2\sqrt{2\pi k_0}}\,T_0\,C'\left(M,-\theta_m^t,\theta_m^i,\rho,\phi\right) \tag{16}$$

2.3. $\pi-\alpha<\phi'<\pi$

The waves penetrate into the wedge through S_0 and S_n, and travel outwards from the apex undergoing reflections/transmissions. Accordingly, the solutions proposed for the case B can be used for the waves penetrating each surface.

3. NUMERICAL RESULTS

Figure 2 shows the results concerning a wedge characterized by $\varepsilon_r=3$ and $\alpha=20°$ when illuminated by a plane wave impinging at $\phi'=35°$. The field magnitude is collected on a circular path with $\rho=4\lambda_0$, λ_0 being the free-space wavelength. In addition to the boundaries related to the incident and specular reflection directions, three GO boundaries exist in the external region (see Fig. 2(a))

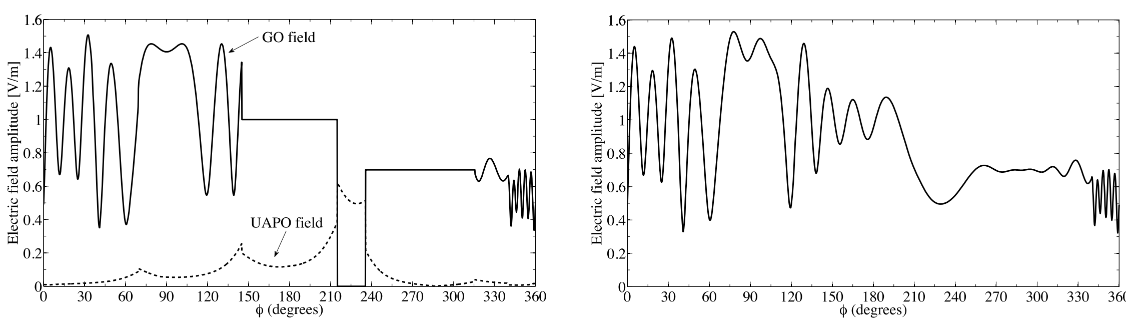

(a) (b)

Figure 2: Electric field amplitude.

since the total internal reflection occurs at the fourth interaction. As can be seen in Fig. 2b, the total field is continuous, thus confirming that the UAPO diffracted field (see Fig. 2(a)) is able to compensate the GO discontinuities. Note that the use of a PO approximation implies inaccuracies at the dielectric interfaces.

REFERENCES

1. Gennarelli, G. and G. Riccio, "A uniform asymptotic solution for diffraction by a right-angled dielectric wedge," *IEEE Trans. Antennas Propagat.*, Vol. 59, 898–903, 2011.
2. Gennarelli, G. and G. Riccio, "Plane-wave diffraction by an obtuse-angled dielectric wedge," *J. Opt. Soc. Am. A*, Vol. 28, 627–632, 2011.
3. Gennarelli, G. and G. Riccio, "Time domain diffraction by a right-angled penetrable wedge," *IEEE Trans. Antennas Propagat.*, Vol. 60, 2829–2833, 2012.
4. Gennarelli, G. and G. Riccio, "Obtuse-angled penetrable wedges: a time domain solution for the diffraction coefficients," *Journal of Electromagnetic Waves and Applications*, Vol. 27, 2020–2028, 2013.
5. Gennarelli, G., M. Frongillo, G. Riccio, "High-frequency evaluation of the field inside and outside an acute-angled dielectric wedge," *IEEE Trans. Antennas Propagat.*, Vol. 63, No. 1, 374–378, 2015.
6. Kouyoumjian, R. G. and P. H. Pathak, "A uniform geometrical theory of diffraction for an edge in a perfectly conducting surface," *Proc. of IEEE*, Vol. 62, 1448–1461, 1974.